The Cryosphere Discuss., doi:10.5194/tc-2016-137, 2016
Manuscript under review for journal The Cryosphere
Published: 12 July 2016

The Cryosphere Discussions
Open Access
EGU

Combined diurnal variations of discharge and hydrochemistry of the Isunnguata Sermia outlet of the Greenland Ice Sheet give insight on subglacial conditions

Joseph Graly, Joel Harrington, Neil Humphrey

University of Wyoming

Abstract

In order to examine daily cycles in meltwater routing and storage in the Isunnuguata Sermia outlet of the Greenland Ice Sheet, variation in outlet stream discharge and in major element hydrochemistry were assessed over a six day period in July, 2013. Discharge was assessed from hourly photography of the outlet from multiple vantages, including where mid-stream naled ice provided a natural gauge. pH, electrical conductivity, suspended sediment, and alkalinity were measured in samples of stream water collected every three hours. Element and ion concentrations were subsequently measured in a laboratory setting.

Photography and stream observations reveal that although river width and stage have only slight diurnal variation, there are large changes in discharge shown in the portion of the width characterized by standing waves and fast flow. Width of this active channel approximately doubles over a diurnal cycle. Together with changes in flow over the naled, these features allow an observationally based relative record of stream discharge in this unconstrained alluvial setting. Peaks in discharge were offset by 3-7 hours from peak melt of the interior ice surface.

Concentration of dissolved solutes follows a sinusoidal diurnal cycle, except for large and variable increases in dissolved solutes during the stream's waning flow. Diurnal changes in solute concentration average 31% of the base value. Diurnal solute concentration minima and maxima lag peak and minimum stream discharge by 3-6 hours.

This phase shift between discharge and solute concentration suggests that during high flow, water is either encountering more rock material or is stored in longer contact with rock material. We

The Cryosphere Discuss., doi:10.5194/tc-2016-137, 2016
Manuscript under review for journal The Cryosphere
Published: 12 July 2016

suggest that expansion of a distributed subglacial hydrologic network into seldom accessed regions during high flow could account for these phenomena, and for a spike of partial silicate reaction products during waning flow, which itself suggests a pressure threshold-triggered release of stored water.

1. Introduction

Dissolved load in glacial outlet streams has long been employed as a metric for assessing water-rock interactions occurring beneath glaciers and ice sheets. Glacierized basins have comparable dissolved loads to non-glacial rivers, but are enriched in mobile cations and depleted in Si (Anderson et al., 1997). Chemistry of glacial water suggests that observed solute concentrations are reached due to presence of reactive accessory minerals and fresh mineral surfaces in glacial sediments (Drever and Hurcomb, 1986). Dissolved load is therefore linked to physical erosion in subglacial environments (Anderson, 2005). Dissolved load is also indicative of the degree to which atmospheric gases have been sequestered by chemical processes in the subglacial environment (Hodson et al., 2000).

Diurnal variation of solute concentration is a potential indicator of meltwater routing and storage. Solute concentration is controlled by total water-rock contact during water residence time in the subglacial environment and by reactivity of minerals contacted by the water. In particular, two end member cases are expected: if dilution produces an inverse relationship between discharge and solute concentration, minimal changes in water-rock interaction over time are suggested, whereas if increased discharge is coupled to increased solute concentration, diurnal changes in processes of water-rock interaction or storage are suggested.

Studies of alpine glaciers have typically found solute concentration and discharge to vary inversely, with rising discharges corresponding to falling concentrations of dissolved solutes (Collins, 1995; Hindshaw et al., 2011; Tranter et al., 1993). Ions produced by saturation limited reactions, such as calcite dissolution, can show increased load with discharge, but typically with diminished concentration

The Cryosphere Discuss., doi:10.5194/tc-2016-137, 2016
Manuscript under review for journal The Cryosphere
Published: 12 July 2016

per water volume (Mitchell and Brown, 2007). Elements that are limited by factors such as the rate of sorption/desorption will have constant flux levels and will only be diluted by increased water flow (Mitchell and Brown, 2007). Resultantly, correlations between discharge and dissolved load are typically weak (Collins and MacDonald, 2004). These dilution relationships have been attributed to the dominance of conduit flow in alpine environments. In cases where subglacial water is confined to fixed conduits, increased water flow will expand the size of these conduits and the speed of through-flow but will have a minimal impact on the area of water-bed contact (Nye, 1976; Röthlisberger, 1972).

Studies of larger glacial systems suggest more complex water-rock interactions. In the outlet of a large glacierized basin in SE Alaska, increases in dissolved load lag spikes in discharge by several days (Anderson et al., 2003). Anderson and others attribute this to storage of water in a distributed system only released during the waning stages of flow. In distributed or linked-cavity flow, increased discharge allows flowing water to spread out across the glacier's bed and thereby increase the area of water-bed contact (Humphrey, 1987; Kamb, 1987). Time series data from the Watson River, near Kangerlussuaq, West Greenland, show out of phase variation in discharge and solute concentration, with maximum daily solute concentrations occurring as discharge is rising and minima occurring as discharge is falling (Yde et al., 2014). However, on the scale of the melt season as a whole, Yde and others find a strong inverse correlation between discharge and solute concentration, which they attribute to conduits carrying a substantially higher portion of the meltwater flow than the distributed subglacial system. Lags between minimum discharge and peak solute concentrations are also observed at Tsanfleuron Glacier, Swiss Alps (Zeng et al., 2012).

Seven measurements of dissolved solute chemistry taken from samples collected over the course of 2 days in 2011 at the terminus of a major west Greenland outlet glacier potentially show a direct relationship between solute concentration and discharge (Graly et al., 2014; Landowski, 2012). In this limited time series, solute concentration appears to peak at midafternoon, while discharge is high,

The Cryosphere Discuss., doi:10.5194/tc-2016-137, 2016
Manuscript under review for journal The Cryosphere
Published: 12 July 2016

and be minimal in the early morning hours, with total variation of <20%. To further investigate whether a direct relationship between discharge and solute concentration exists in the Isunnguata Sermia outlet of the western Greenland Ice Sheet, we returned to the same site for a six day period of the summer of 2013, collecting 8 samples per day for chemical analysis.

2. Field site

Water samples were collected from the terminus of Isunnguata Sermia, a major land-terminating outlet of the western Greenland Ice Sheet (Figure 1). The outlet glacier Isunnguata Sermia occupies a deeply cut glacial valley, with surrounding hilltops >400 m above sea level. Deep, glacially-carved trenches continue under the ice sheet for more than 20 km into interior, with ice depths of greater than 1,000 m (Jezek et al., 2013). The Isunnugata Sermia outlet has a catchment that encompasses >2,400 km^2 of the ablation zone, making it one of the largest regional subglacial drainage basins (Palmer et al., 2011). Regional geology consists of primarily of Paleoproterozoic gneisses and granitoids (van Gool et al., 2002). The Isunnguata Sermia outlet is located 25 km from the town of Kangerlussuaq. It is the next outlet to the north of the Russell Glacier and feeds a separate glacial river system from the Watson River.

Water emerges from a single location on the south side of Isunnguata Sermia's terminus front ~30m above sea-level (Figure 1) and traverses a broad, >100 km long sandur to the fjord. Discharge of pressurized subglacial water creates a large upwelling capable of expelling water multiple meters into the air and, although no fully quantitative measurement could be made, peak discharge was estimated to exceed 500 m^3s^{-1}. Ice-cored moraines and frozen outwash shape the course of outlet waters. On the sandur, frozen outwash channels the water into a single thread, although the large sediment load creates rapidly changing channel and bed geometry. Near the terminus, the frozen outwash of the sandur is elevated ~2-4 meters above the discharging stream. The main stream is also fed by minor ice

The Cryosphere Discuss., doi:10.5194/tc-2016-137, 2016
Manuscript under review for journal The Cryosphere
Published: 12 July 2016

surface melt streams. A small stream that runs along the south lateral margin of the glacier joins the main terminal outlet stream just below the primary upwelling site.

This work was performed in the context of several other studies of the Isunnguata Sermia terminus. Hot water boreholes along a transect from the outlet to 40 km in the interior have provided data regarding water pressure (Meierbachtol et al., 2013), ice temperature (Harrington et al., 2015), subglacial water chemistry (Graly et al., 2014), and mass balance between subglacial sediment and rock (Graly et al., 2016). More limited datasets from Isunnguata Sermia's terminal and lateral outlets were reported for the 2010, 2011, and 2012 seasons (Graly et al., 2014). The work reported here is based on samples and data collected over a 6 day period from July 16th to July 21st, 2013.

3. Methods

3.1 Water Sampling

Water sampling began at 8:00 hours local time on July 16th, 2013 and continued in 3 hour increments through 20:00 hours on July 21st, 2013. Samples were collected by lowering a liter bottle attached to a pole into discharging waters within 400 m of the subglacial upwelling. During July 16th and July 17th, samples were collected from the south bank of the outlet stream from the banks at the beginning of the outwash plain (Figure 1). During July 17th, the main course of the river shifted so that location had diminished flow and an emerging bank channeled waters from the lateral side stream to the location. Commencing at 14:00 hours on July 18th, sampling was relocated above the lateral side stream on the banks of the terminal moraine (Figure 1). The sampling location was not subsequently changed. Excepting periods where the emerging bank channeled lateral stream water to the first location, both locations sampled water from the main subglacial outlet and should produce comparable results.

The Cryosphere Discuss., doi:10.5194/tc-2016-137, 2016
Manuscript under review for journal The Cryosphere
Published: 12 July 2016

120 Upon collection, 125 ml of water sample were pumped through 0.1 µm nylon filters, with
121 filtered water and filter papers saved for laboratory analyses. A colorimetric alkalinity test, a
122 conductivity measurement, and a pH measurement were performed on the remaining unfiltered
123 sample. Alkalinity tests were performed with a Hach Model AL-AP alkalinity test kit. Results of field
124 alkalinity tests were only accurate to 25 µM. Alkalinity was therefore also calculated by charge balance
125 from the other measured ions. pH measurements and conductivity measurements were performed with
126 Beckman-Coulter Φ460 multi-parameter meter. pH was measured using a low ionic strength probe.
127 Subsequent water analyses were performed in the University of Wyoming Aqueous
128 Geochemistry Lab. Concentrations of Si, Ca, Mg, Na, and K were measured on a Perkin Elmer Elan 6000
129 inductively coupled plasma quadrupole mass spectrometer (ICP-MS). Concentrations of SO_4^{2-}, Cl^-, NO_3^-,
130 and Fl^- were measured on a Dionex ICS 500 ion chromatograph. The filter papers were dried and
131 weighed to assess suspended load.
132
133 **3.2 Discharge**
134 Discharge measurements of the outlet were difficult. There is no exposed bedrock near the
135 stream to act either as an elevation reference or to stabilize the river bed. Obtaining accurate cross
136 profiles of the stream was prohibitively dangerous, with high flows, collapsing banks, and a considerable
137 flux of mobile ice blocks. Attempts to install a stage pole were frustrated by considerable stage variation
138 over time associated with cutting and filling of the river bed and banks. Once the stream opens out from
139 its restriction by remnant glacier ice near the upwelling, stage is poorly correlated with discharge. The
140 stream instead scours sediment during the rising limb and deposits it on the trailing limb of the daily
141 hydrograph. It was decided to assess only relative discharge. This was aided by repeat photography from
142 two fixed locations.

The Cryosphere Discuss., doi:10.5194/tc-2016-137, 2016
Manuscript under review for journal The Cryosphere
Published: 12 July 2016

143 Hourly stream photography began at 10:00 hours on July 18th and continuing through 20:00
144 hours on July 21st. From one vantage point, the central upwelling of subglacial water was photographed
145 from the south, as it poured out from around the moraine. This vantage captured a ~1 meter high, mid-
146 channel naled formed from freezing of outlet waters during winter months. The naled was variably
147 covered or exposed as discharge varied and acted as a stream gauge in this respect. This portion of the
148 stream is restricted by frozen sediment and stream height is controlled by discharge.
149 A second vantage, from a rise above the south bank, captured a ~200m long stretch of the
150 outlet stream. In this portion of the stream, increased discharge caused scour and expansion of the
151 stream's active channel. Photography allowed assessment of relative active channel width. Large waves
152 and faster velocities are confined to this active channel, allowing fairly unambiguous, though qualitative,
153 determination of which portions of an overhead photograph comprise the active channel. The distance
154 between the upstream end of a persistent, mid-stream point bar and a distinct feature on the south
155 shore was measured on each photograph (Figure 1). The length of the portion of this transect
156 characterized by large waves and flow features was also measured, allowing for the calculation of the
157 percentage of the stream width contained by the active channel. The second vantage also allowed
158 assessment of flow state and Froude number from the presence of features such as standing waves.
159 During the first two days of the sampling period, stream surface velocity was measured by
160 repeated timing the motion of floating ice and other stream surface features down a 100 m section of
161 the stream. Measurements were taken during morning, afternoon, and evening stages to assess
162 variation in velocity associated with high and low flow.
163
164 **3.3 Interior Surface Melt**
165 In order to compare variation in terminus discharge to melt in the surface interior, we are also
166 including discharge measurements from an interior ice sheet surface stream. The stream was gauged

The Cryosphere Discuss., doi:10.5194/tc-2016-137, 2016
Manuscript under review for journal The Cryosphere
Published: 12 July 2016

167 during the summer of 2012, so data are not directly comparable to the measurements collected in 2013.
168 However inasmuch as interior melt is primarily controlled by insolation, the stream's variation likely
169 represents a typical pattern for the timing and scaling of diurnal summer surface melt fluctuations.

170 The surface stream was located at 67.2˚N and 49.8˚E, ~25 km from the terminal outlet. Stream
171 height was gauged with a calibrated pole drilled into ice. Surface velocity was measured by timing
172 floating ice along a course of known distance. Cross-sectional area was directly measured in the region
173 where the gauge was emplaced and calibrated to gauge height. Transect slope was measured by pole
174 and automatic level. Six measurements of surface velocity used to calculate an average Manning
175 coefficient from the measured slope and hydraulic radius of the stream. Discharge was then calculated
176 from change in gage height. Stage height was measured every half hour or hour for a period from 11:30
177 6/18/12 to 20:00 6/21/12. During June 18th, 19th, and 20th, sunny weather predominated; June 21st had
178 rainy, cooler weather.

179

180 **4. Results**

181 **4.1 Discharge**

182 Over the four days during which repeat photographic observations were made, photographs of
183 the naled show consistent minima at 8:00 hours, with the naled is mostly exposed, and a small volume
184 of water overtopping a portion of the ice body (Figure 2). During the first two days of observation, the
185 naled was completely covered by flowing water from 19:00 to 0:00 hours. On the third day it was
186 covered from 16:00 hours, and remained covered for the remainder of the study period.

187 Maximum discharge is harder to determine from observations of the naled alone. Once the
188 naled is completely covered in water, visual interpretation of maximum flow is ambiguous. Some
189 discrimination can be made based on height of the covered naled feature compared to the surrounding
190 waves and angle at which the water pours over the naled (greater flows overtop the naled at a lower

The Cryosphere Discuss., doi:10.5194/tc-2016-137, 2016
Manuscript under review for journal The Cryosphere
Published: 12 July 2016

191 angle). From these features, maximum stream flow appears to occur at 21:00 hours on July 18th and
192 19th, and 20:00 hours on July 20th.

193 Standing waves are observed at all flows (Figure 2), although substantial differences in wave and
194 surface morphology were noted during waxing and waning phases, with rougher water in waning flow
195 and smoother water in waxing flow. The roughness change may represent a change in the sediment load
196 of the river between the erosive waxing stage and the depositional waning stage. The persistence of
197 standing waves implies near critical flow conditions, or a Froude number approximately 1, for the entire
198 study period. Measurements of stream velocity showed surface speeds of 2.86 ± 0.12 m/s (2σ, n=6).
199 Variation in velocity between morning and evening stages was within measurement error. Based on
200 calculations from a Froude number of 1, stream depths of 0.5 - 0.9 m are suggested; these depth
201 estimates were supported by observing ice blocks rolling or bouncing down the flow. The lack of
202 relationship between stage and discharge and velocity has been noted before in sediment laden glacial
203 rivers (Humphrey and Raymond, 1994).

204 Since neither stream velocity nor depth change with discharge, variations in discharge are
205 accommodated by changes in the width of the active channel. Wide areas of shallow slow water
206 remained present during low flows and the total surface area of the stream remained approximately
207 constant. Pole probing of these shallow areas suggests 10 to 20 cm depths. Because the active channel
208 has an order of magnitude greater discharge per transect meter than the marginal areas and changes in
209 active channel water velocity were not observed, cross-sectional area of the active channel is the
210 primary control on discharge.

211 Assessment of the active channel width shows substantial differences between morning hours
212 (~5:00-10:00), where 20-30% of the stream is comprised of active channel characteristics, and late
213 afternoon / evening hours (~18:00-0:00) where >40% of the stream is comprised of active channel

The Cryosphere Discuss., doi:10.5194/tc-2016-137, 2016
Manuscript under review for journal The Cryosphere
Published: 12 July 2016

214 characteristics. These observations are generally consistent with assessments of the height of water
215 pouring over the naled (Figure 3).
216
217 **4.2 Interior Surface Stream**
218 The calculated Manning coefficient for the interior stream was 0.0117 ± 0.0018 (2σ). Discharge
219 measured in the interior ice surface stream varied by as much as an order of magnitude during the
220 course of diurnal cycles, with low values as small as 0.3 m^3s^{-1} and high values greater than 3.5 m^3s^{-1}
221 (Figure 3). Minimum stage heights consistently occurred around 4:00 hours. Maximum stage heights
222 consistently occurred at 14:00 or 15:00 hours. These data contrast with our observations of water
223 pouring over the naled. The naled minimum occurred approximately 4 hours later than minimum of
224 surface melt. The naled maximum occurred approximately 6 hours later than maximum surface melt.
225 This delay is representative of the integration of the travel time delays from the entire glacier
226 catchment.
227
228 **4.3 Water Analyses**
229 Sampled waters are generally chemically dilute, with 292±50 micromoles per liter dissolved
230 solutes (Table 1). Ca is the dominant cation, followed by Na, K, and Mg (Figure 4). Mg abundances are an
231 order of magnitude lower than the other major cations. Dissolved Si occurs at comparable abundance to
232 Na. Standard deviations of the mass spectrometer measurements were <1% of the measured value.
233 Bicarbonate (measured as alkalinity) is the dominant anion. SO_4^{2-} and Cl^- are detected in all samples, but
234 occur at an order of magnitude lower concentration. Trace amounts of NO_3^- and Fl^- were detected in
235 some samples, at values an order of magnitude below SO_4^{2-} and Cl^- concentrations (Figure 4). On
236 average, field alkalinity measurements exceed the alkalinity estimates from charge balance by 25 ± 14
237 µM (2σ). Some over-measurement in the field titration is expected, as the value is recorded at the level

The Cryosphere Discuss., doi:10.5194/tc-2016-137, 2016
Manuscript under review for journal The Cryosphere
Published: 12 July 2016

where the color tracer disappears (and therefore is a maximum compared to previous drop). Charge imbalance may also result from absorption of H^+ particles to suspended sediment in unfiltered water. Field electrical conductivity measurements show similar results to the laboratory analyses ($p<0.0001$) (Figure 4). Suspended sediment concentration does not show a consistent correlation or anti-correlation with dissolved load (Figure 4).

Relative abundances of cation species is comparable to measurements taken at the Isunnguata Sermia terminus in the summer of 2011 (Graly et al., 2014). The SO_4^{2-}/alkalinity ratios are diminished compared to those measured in 2011, but are comparable to those found in samples collected in 2010 and 2012. The concentrations of suspended sediment are similar to those observed at nearby Leverett Glacier during the summer of 2010 (Cowton et al., 2012).

When normalized to average concentration, magnitude and timing of cation and silica concentration variation is highly consistent between species over time (Figure 5). Covariation of all cation and Si species is statistically significant with $p<0.05$. Covariations of K-Mg, K-Si, and Na-Si have p-values ranging from 0.01 to 0.05; all others are <0.0001. All cations and silica concentrations follow a diurnal pattern with higher concentrations during morning and early afternoon hours and significantly lower concentrations during later afternoon and evening hours. In several of the studied cycles, large changes in total concentration are limited to the 20:00 and 23:00 hours samples, which are substantially lower than the other samples collected throughout the day.

There are two major deviations from the diurnal pattern. The 11:00, 14:00, 17:00, and 20:00 samples from July 17th have substantially lower concentrations than would be otherwise suggested by diurnal fluctuations observed elsewhere in the record. This corresponds with the period during which an emerging bank partially separated site 1 from the main channel allowing a surface-fed side stream to substantially dilute the water.

The Cryosphere Discuss., doi:10.5194/tc-2016-137, 2016
Manuscript under review for journal The Cryosphere
Published: 12 July 2016

261 At 2:00 on July 20th, there is a >60% spike in total concentration of all cations. Similar, but
262 smaller magnitude spikes are also present in the 2:00 samples of July 19th and 21st and the July 16th
263 23:00 sample. The most clearly expressed of these spikes (July 20th and 21st) are substantially more
264 expressed in Na and K concentrations than in Ca, Mg, or Si. During the July 21st spike, the spike in Mg
265 and Si appears to proceed the spike in Ca, Na and K in that it appears during the previous sampling
266 period. Large variability in the magnitude of these spikes suggests that the 3-hour sampling schedule
267 was insufficiently frequent to characterize them entirely.

268 Anions generally follow similar patterns, but with greater variability (Figure 4). In particular, Cl
269 does not co-vary with other ions toward the end of the record. The spike on July 18th coincides with a
270 drop in SO_4 concentration; the spike on the 20th coincides with a drop in Cl concentration. SO_4
271 concentrations generally only minimally increase during the spikes.

272 Excluding these anomalies, the highest concentration of dissolved solids occurs at 11:00 on July
273 16th, 19th, 20th, and 21st (Figure 5). On July 17th and 18th, the 11:00 sample was likely diluted by the side
274 stream (which was a significant component of flow to site 1 during that period). Concentration minima
275 are reached at 23:00 hours on July 17th through 20th. On July 16th, the minima occurs in the 20:00
276 sample. The size of the diurnal variation varies from 22% to 49% of the lowest value, with an average
277 daily range of 31 ± 9%.

278

279 **5. Discussion**

280 *5.1 Discharge and Outlet Stream Observations*

281 Observations from oblique photography suggest large diurnal changes in discharge. Width of the
282 active channel, with deeper faster water, approximately doubles in the course of the day (Figure 3b). An
283 approximate doubling of discharge is also suggested by observations of the midstream naled. The naled
284 is of comparable scale to the depth of the stream (both order of 1 meter). Its exposure during low flow

The Cryosphere Discuss., doi:10.5194/tc-2016-137, 2016
Manuscript under review for journal The Cryosphere
Published: 12 July 2016

and burial during high flow suggests a change in stage comparable to its height. At the naled site, increased width of active channel flow is restricted by ice. Increases in flow height at the naled location are therefore approximately equivalent to increases in active channel width downstream.

During high flows, diurnal increases in discharge of up to 50% of base value are observed in the Watson River at Kangerlussuaq, where a bridge over a narrow gorge has allowed for the construction of a reliable gauge (Hasholt et al., 2013). As the Watson River is 20-30 km from its glacial outlet sources and integrates several independent glacial outlet streams, these diurnal cycles are likely muted compared to their expression at the ice margin. Larger diurnal changes are therefore expected directly at glacier outlet termini. Contrastingly, Smith and others (2015) found minimal diurnal variation in discharge at Isunnguata Sermia terminus. However, as Smith and others estimated discharge based solely on the surface area of the outlet stream water, their analysis missed the variation in the width of the active channel and height of its flow over static features that we present.

5.2 Diurnal Changes in Solute Flux

The critical observation is that variability in the dissolved solute concentrations cannot be explained by dilution alone. First, the scale of discharge variation is substantially larger than variation in concentration of dissolved solutes. Approximate width of the main channel doubles during diurnal cycles, while concentrations of dissolved solutes only change by an average of 21-40% (Figure 5). Secondly, maximum and minimum solute concentrations are offset from minimum and maximum discharge. Such lags imply periods where solute concentration is increasing even as discharge rises and periods where solute concentration is falling even as discharge falls.

Periods of in-phase changes between discharge and solute concentration suggest that increased water flow is either stimulating increased water-rock interaction or allowing for release of stored water (that has developed higher solute concentrations over longer residence times). While the single

The Cryosphere Discuss., doi:10.5194/tc-2016-137, 2016
Manuscript under review for journal The Cryosphere
Published: 12 July 2016

upwelling structure of the terminus of Isunnguata Sermia implies local channelized flow, observations of water pressures at interior sites (Meierbachtol et al., 2013) and hydrologic theory for low ice surface slopes (Werder et al., 2013) both suggest that much of the catchment interior has a linked-cavity flow system. Linked cavity systems would allow for expansion of the basal hydrological system and flushing of long water residence time regions under high flow conditions.

Sudden increases in solute concentration during waning flow suggest that discharge from subglacial regions with a high concentration of dissolved solutes is triggered when a threshold is reached. Multiple triggering mechanisms are plausible. Modeling of subglacial water pressures suggests that near the ice sheet margin, water flows from conduits to the distributed cavity system at high conduit water pressures and back to conduits at low pressures (Meierbachtol et al., 2013). Solute concentration spikes result from the crossing of a pressure threshold allowing water stored during high flow to suddenly enter the glacial outlet system.

Solute concentration spikes might also be explained by creep closure of linked cavities that opened during high flow and expulsion of remaining solute-concentrated water. Anderson and others (2003) proposed a similar creep closure mechanism to explain increases in solute concentration during waning flow that occurred on a multiday scale in a mountain glacier setting. Following the Glenn-Nye relation, the rate of creep closure of ice scales to approximately the third power of effective pressure (Cuffey and Paterson, 2010). Differences in timing of these effects between ice sheets and mountain glaciers can therefore be explained by differences in ice thickness.

Relative dominance of Na and K in these spikes is consistent with water-rock interactions occurring only over a limited time, such that cation exchange occurred on fresh feldspar and mica surfaces but complete silicate dissolution and clay precipitation did not (Blum and Stillings, 1995; Graly et al., 2014). Contrastingly, constituents associated with weathering of reactive accessory minerals such as pyrite and calcite (especially SO_4) are minimally expressed. This implies that the spikes' composition

The Cryosphere Discuss., doi:10.5194/tc-2016-137, 2016
Manuscript under review for journal The Cryosphere
Published: 12 July 2016

reflects waters that have rapidly passed through reactive sediment that is depleted of accessory minerals. Such accessory mineral depletion can occur if sediment residence time in the subglacial system is sufficiently long (Graly et al., 2014). Sampling of sediment beneath ice boreholes has shown the greatest chemical depletion in portions of the ice sheet most likely to be influenced by distributed flow (Graly et al., 2016). This suggests that the spike of chemical solutes comes from water that has temporarily entered regions of distributed flow as a part of a diurnal cycle.

6. Conclusions

A semi-quantitative discharge record can be constructed through hourly photographic monitoring of the static and dynamic features of a large, sediment laden glacial outlet stream. These assessments show large diurnal changes in discharge over the six day study period at the Isunnguata Sermia outlet of the Greenland Ice Sheet (c.f. Smith et al., 2015). Simultaneously collected chemical measurements show substantially smaller fluctuation in dissolved load; thus this Greenland outlet glacier does not show the discharge-driven dilution of solute concentration that is common in smaller ice masses. Periods where dissolved solute concentration increase and decrease along with discharge, and abrupt and variable increases in solute concentration during waning flow imply that significant contributions to the solute load is made by changes to the routing and storage of meltwater in the subglacial system over the course of the day. In particular, these results indicate considerable exchange of water diurnally between the conduit and linked cavity drainage systems, as well as implying threshold pressure conditions for these exchanges.

*Acknowledgements.*This work would not have been possible without funding from the Greenland Analogue Project (SKB, Posiva, NWMO) and NSF grant ARC-0909122. Janet Dewey assisted with laboratory analyses.

The Cryosphere Discuss., doi:10.5194/tc-2016-137, 2016
Manuscript under review for journal The Cryosphere
Published: 12 July 2016

357

358 **Cited References**

359 Anderson, S.P., 2005. Glaciers show direct linkage between erosion rate and chemical weathering fluxes.
360 Geomorphology 67, 147-157.
361 Anderson, S.P., Drever, J.I., Humphrey, N.F., 1997. Chemical weathering in glacial environments. Geology
362 25, 399-402.
363 Anderson, S.P., Longacre, S.A., Kraal, E.R., 2003. Patterns of water chemistry and discharge in the
364 glacier-fed Kennicott River, Alaska: Evidence of subglacial water storage cycles. Chemical Geology
365 202, 297-312.
366 Blum, A.E., Stillings, L.L., 1995. Feldspar dissolution kinetics, in: White, A.F., Brantley, S.L. (Eds.),
367 Chemical Weathering Rates of Silicate Minerals. Mineralogical Soc Amer, Chantilly, pp. 291-351.
368 Collins, D., 1995. Dissolution kinetics, transit times through subglacial hydrological pathways and diurnal
369 vatiations of solute content of meltwaters draining from an alpine glacier. Hydrological Processes 9,
370 897-910.
371 Collins, D.N., MacDonald, O.G., 2004. Year-to-year variability of solute flux in meltwaters draining from a
372 highly-glacierised basin. Nordic Hydrology 35, 359-367.
373 Cowton, T., Nienow, P., Bartholomew, I., Sole, A., Mair, D., 2012. Rapid erosion beneath the Greenland
374 ice sheet. Geology 40, 343-346.
375 Cuffey, K.M., Paterson, W.S.B., 2010. The Physics of Glaciers, 4th ed.
376 Drever, J.I., Hurcomb, D.R., 1986. Neutralization of atmospheric acidity by chemical weathering in an
377 alpine drainage basin in the North Cascade Mountains. Geology 14, 221-224.
378 Graly, J.A., Humphrey, N.F., Harper, J.T., 2016. Chemical depletion of sediment under the Greenland Ice
379 Sheet. Earth Surface Processes and Landforms In Press.

380 Graly, J.A., Humphrey, N.F., Landowski, C.M., Harper, J.T., 2014. Chemical weathering under the
381 Greenland Ice Sheet. Geology 42, 551-554.
382 Harrington, J., Humphrey, N.F., Harper, J.T., 2015. Temperature distribution and thermal anomalies
383 along a flowline of the Greenland Ice Sheet. Annals of Glaciology 56(70), 98-104.
384 Hasholt, B., Mikkelsen, A.B., Nielsen, M.H., Larsen, M.A.D., 2013. Observations of runoff and sediment
385 and dissolved loads from the Greenland Ice Sheet at Kangerlussuaq, West Greenland, 2007 to 2010.
386 Zietschrift fur Geomorphologie 57, sup. 2, 3-27.
387 Hindshaw, R.S., Tipper, E.T., Reynolds, B.C., Lemarchand, E., Wiederhold, J.G., Magnusson, J.,
388 Bernasconi, S.M., Kretzschmar, R., Bourdon, B., 2011. Hydrological control of stream water
389 chemistry in a glacial catchment (Damma Glacier, Switzerland). Chemical Geology 285, 215-230.
390 Hodson, A., Tranter, M., Vatne, G., 2000. Contemporary rate of chemical denudation and atmospheric
391 CO_2 sequestration in glacier basins: An arctic perspective. Earth Surface Processes and Landforms
392 25, 1447-1471.
393 Humphrey, N.F., 1987. Coupling between water pressure and basal sliding in a linked-cavity hydraulic
394 system, The Physical Basis of Ice Sheet Modelling. IAHS Publ. No. 170, pp. 105-118.
395 Humphrey, N.F., Raymond, C.F., 1994. Hydrology, erosion and sediment production in a surging glacier:
396 Variegated Glacier, Alaska, 1982-83. Journal of Glaciology 40, 539-552.
397 Jezek, K., Wu, X., Paden, J., Leuschen, C., 2013. Radar mapping of Isunnguata Sermia, Greenland. Journal
398 of Glaciology 59, 1135-1147.
399 Kamb, B., 1987. Glacier surge mechansim based on linked cavity configuration of the basal water conduit
400 system. Journal of Geophysical Research 92, 9083-9100.
401 Landowski, C., 2012. Geochemistry and subglacial hydrology of the West Greenland Ice Sheet, MS
402 Thesis, Geology and Geophysics. University of Wyoming.

403 Meierbachtol, T., Harper, J., Humphrey, N., 2013. Basal drainage system response to increasing surface
404 melt on the Greenland Ice Sheet. Science 341, 777-779.
405 Mitchell, A.C., Brown, G.H., 2007. Diurnal hydrological - physicochemical controls and sampling methods
406 for minor and trace elements in an Alpine glacial hydrological system. Journal of Hydrology 332,
407 123-143.
408 Nye, J.F., 1976. Water flow in glaciers: Jokulhlaups, tunnels, and veins. Journal of Glaciology 17, 181-207.
409 Palmer, S., Shepherd, A., Nienow, P., Joughin, I., 2011. Seasonal speedup of the Greenland Ice Sheet
410 linked to routing of surface water. Earth and Planetary Science Letters 302, 423-428.
411 Röthlisberger, H., 1972. Water Pressure in Intra- and Subglacial Channels. Journal of Glaciology 11, 177-
412 203.
413 Smith, L.C., Chu, V.W., Yang, K., Gleason, C.J., Pitcher, L.H., Rennermalm, A.K., Legleiter, C.J., Behar, A.E.,
414 Overstreet, B.T., Moustafa, S.E., Tedesco, M., Forster, R.R., LeWinter, A.L., Finnegan, D.C., Sheng, Y.,
415 Balog, J., 2015. Efficient meltwater drainage through supraglacial streams and rivers on the
416 southwest Greenland ice sheet. Proceedings of the National Academy of Sciences of the United
417 States of America 112, 1001-1006.
418 Tranter, M., Brown, G., Raiswell, R., Sharp, M., Gurnell, A., 1993. A conceptual model of solute aquisition
419 by Alpine glacial meltwaters. Journal of Glaciology 39, 573-581.
420 van Gool, J.A.M., Connelly, J.N., Marker, M., Mengel, F.C., 2002. The Nagssugtoqidian Orogen of West
421 Greenland: Tectonic evolution and regional correlations from a West Greenland perspective.
422 Canadian Journal of Earth Science 39, 665-686.
423 Werder, M.A., Hewit, I.J., Schoof, C.G., Flowers, G.E., 2013. Modeling channelized and distributed
424 subglacial drainage in two dimensions. Journal of Geophysical Research: Earth Surface 118, 1-19.

The Cryosphere Discuss., doi:10.5194/tc-2016-137, 2016
Manuscript under review for journal The Cryosphere
Published: 12 July 2016

425 Yde, J.C., Knudsen, N.T., Hasholt, B., Mikkelsen, A.B., 2014. Meltwater chemistry and solute export from
426 a Greenland Ice Sheet catchment, Watson River, West Greenland. Journal of Hydrology 519, 2165-
427 2179.
428 Zeng, C., Gremaud, V., Zeng, H., Liu, Z., Goldscheider, N., 2012. Temperature-driven meltwater
429 production and hydrochemical variations at a glaciated alpine karst aquifer: implication for the
430 atmospheric CO_2 sink under global warming. Evironmental Earth Science 65, 2285-2297.

431
432

The Cryosphere Discuss., doi:10.5194/tc-2016-137, 2016
Manuscript under review for journal The Cryosphere
Published: 12 July 2016

433 **Figures:**

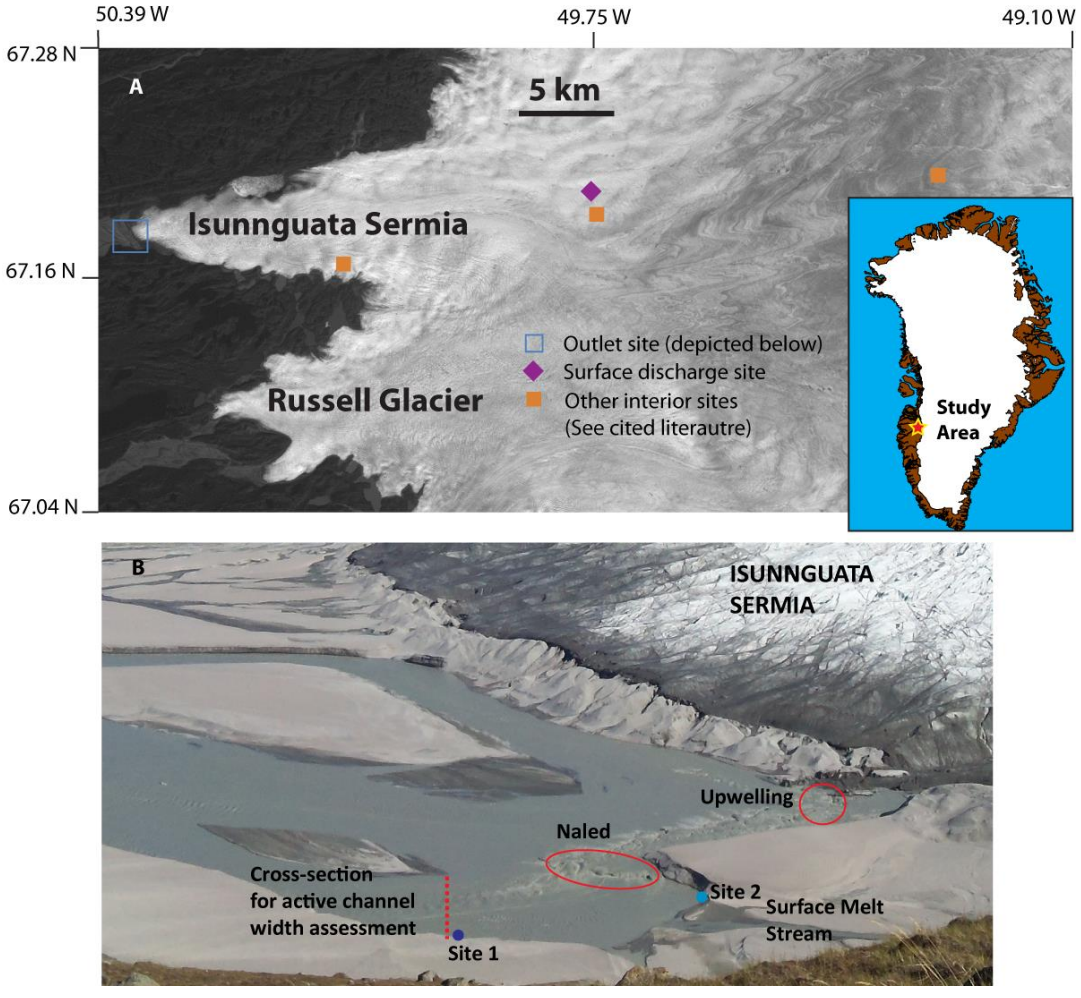

434

435 **Figure 1.** A) Location of the study area. B) Overhead photograph of the study area (taken 7/22/13) with
436 important sampling and observational features. Samples were collected at site 1 from 10:00 hrs on
437 7/16/13 through 11:00 hours on 7/18/13. Samples were collected at site 2 from 14:00 hrs on 7/18/13
438 through 20:00 hrs on 7/22/13. Beginning at 10:00 hrs on 7/18/13, hourly photographs on the labeled
439 naled and ~100 m cross-section were taken.

440

The Cryosphere Discuss., doi:10.5194/tc-2016-137, 2016
Manuscript under review for journal The Cryosphere
Published: 12 July 2016

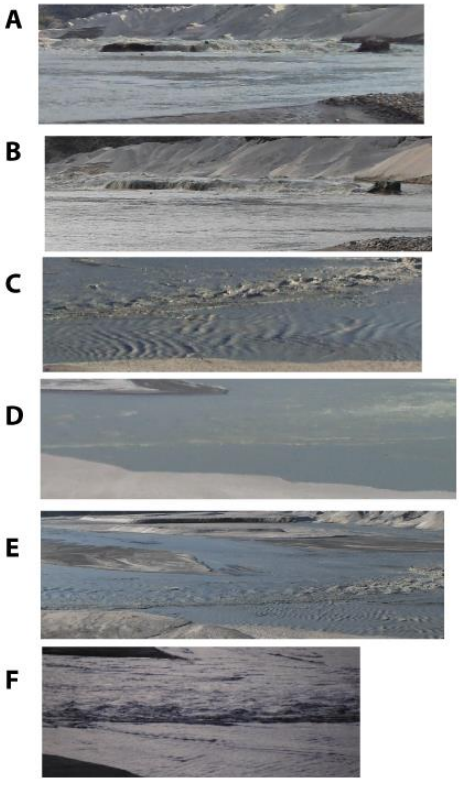

441

442 **Figure 2.** Photographs of typical flow patterns in the Isunnguata Sermia outlet. A) Midstream naled
443 exposed at during low flow (8:00). B) Midstream naled covered during high flow (21:00). C-F show flow
444 during low (8:00), waxing (14:00), high (21:00) and waning (0:00) stages. Waxing and waning stages
445 show different wave morphology but maintain standing wave features.

446

The Cryosphere Discuss., doi:10.5194/tc-2016-137, 2016
Manuscript under review for journal The Cryosphere
Published: 12 July 2016

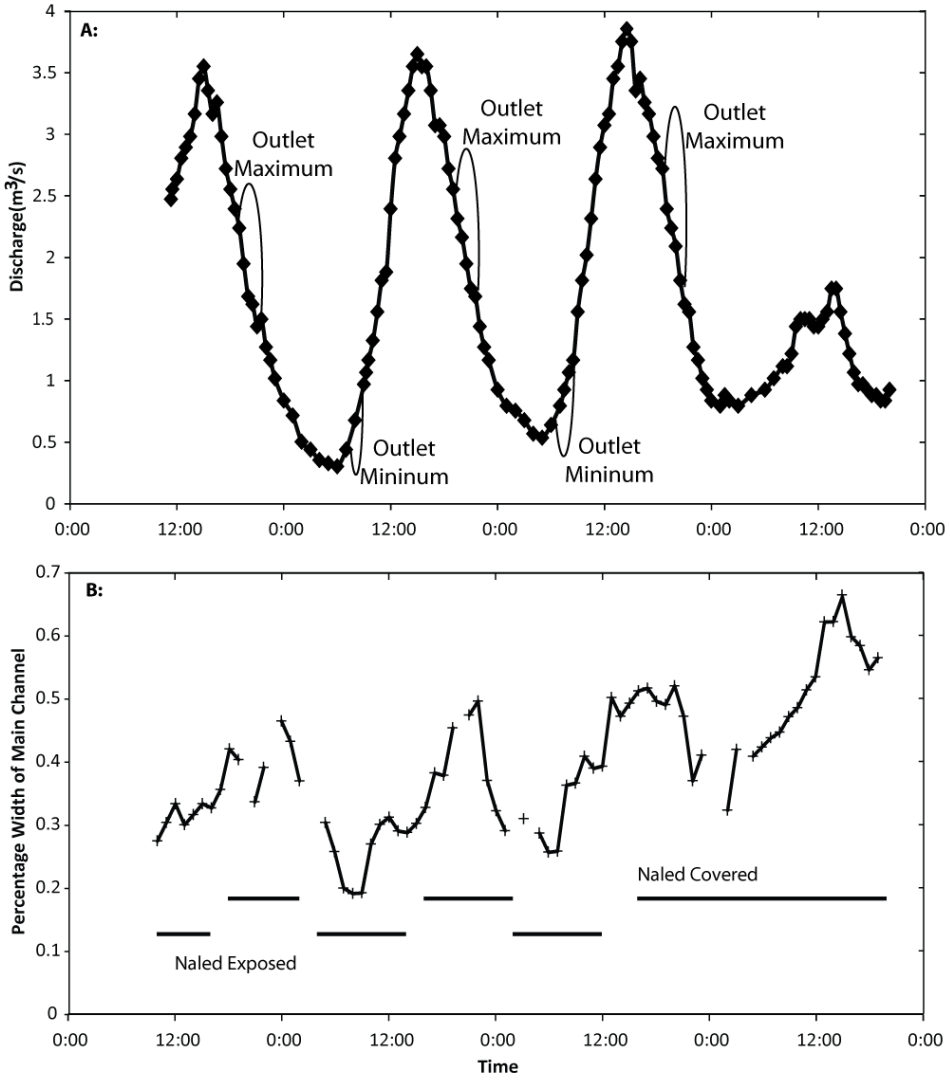

447

448 **Figure 3.** A) Measured discharge in an interior surface stream over a 4 day period in 2012 compared to
449 time ranges of maximum and minimum discharge as suggested by flow volumes over midstream naled
450 ice in the outlet of Isunnguata Sermia during the study period. B) Assessment of percentage of distance
451 between a point bar and the shore that is characterized by large waves suggestive of deep, fast flow.
452 Periods of time where the midstream naled is exposed and covered are included for comparison.

453

The Cryosphere Discuss., doi:10.5194/tc-2016-137, 2016
Manuscript under review for journal The Cryosphere
Published: 12 July 2016

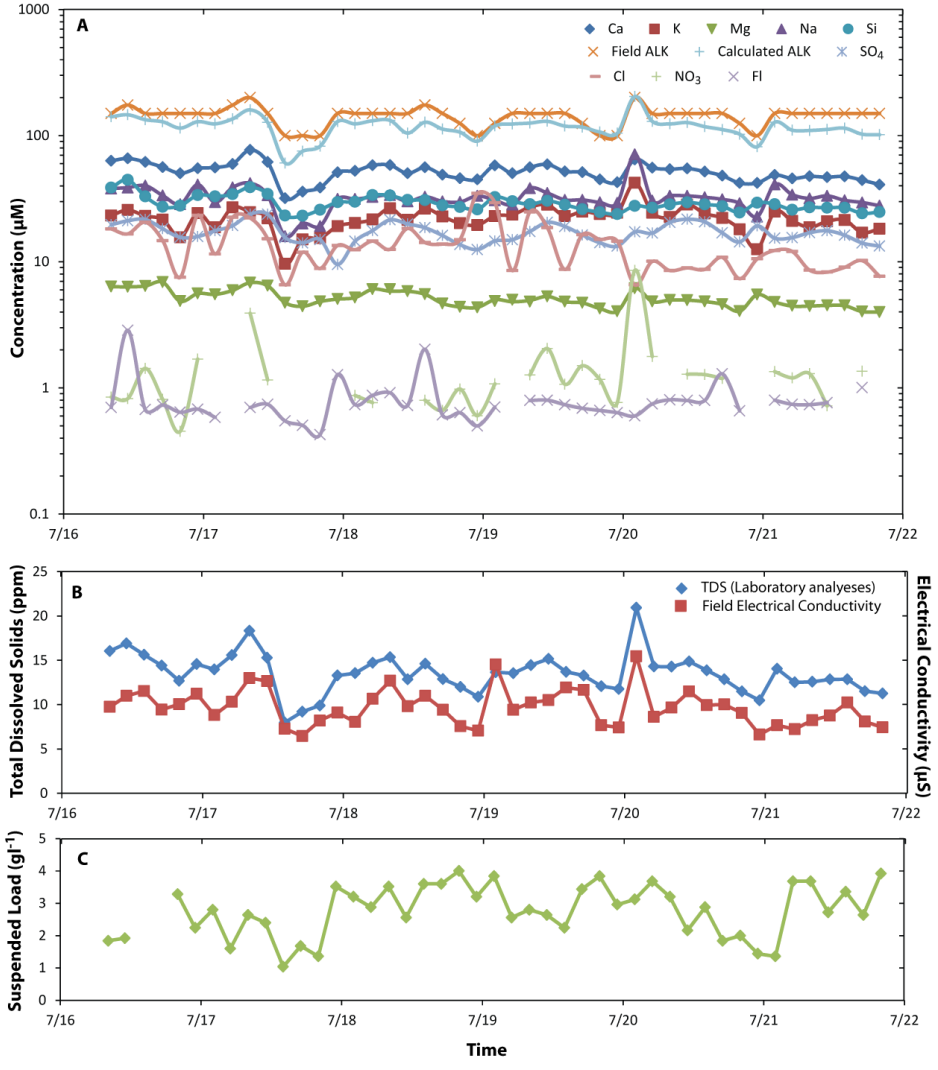

Figure 4. A) Concentration of dissolved constituents in sampled waters over time, including laboratory measurements of cations and Si by ICP-MS, anions by ion chromatography, and field measurements of alkalinity (ALK). Alkalinity as calculated by charge balance is also depicted. B) Total dissolved solids from the sum of the laboratory measurements and charge balance alkalinity (HCO_3) compared to field conductivity measurements. Co-variation is statistically significant ($p<0.0001$). C) Dry weight of suspended sediment on filters.

The Cryosphere Discuss., doi:10.5194/tc-2016-137, 2016
Manuscript under review for journal The Cryosphere
Published: 12 July 2016

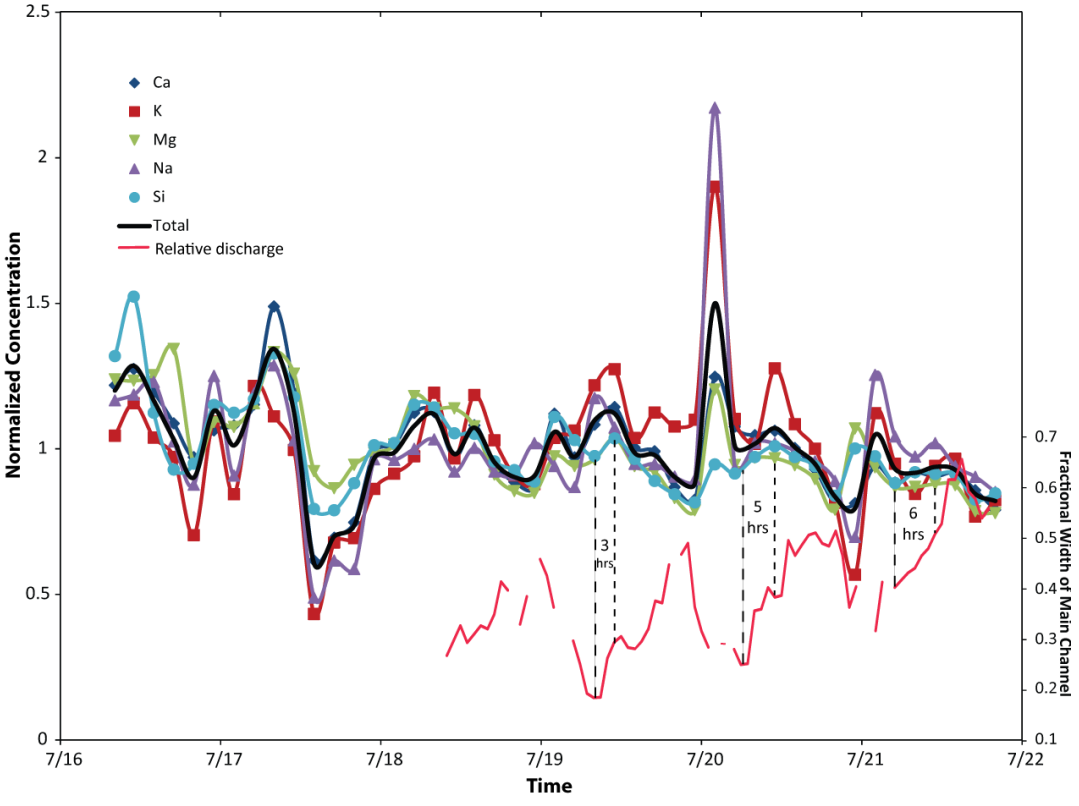

Figure 5. Concentration of dissolved cations and Si normalized to average concentration. Discharge from relative active channel width is shown for comparison. Lags between active channel width channel minima and solute concentration maxima are illustrated with dashed lines.

The Cryosphere Discuss., doi:10.5194/tc-2016-137, 2016
Manuscript under review for journal The Cryosphere
Published: 12 July 2016

466 **Tables:**

467

468 Table 1. Field and laboratory measurements (results in micro-molarity unless otherwise noted)

Sample	Time	pH	Eletrical Conductivity (µS)	Suspended Sediment (gl^{-1})	Field Alkalinity (µM)	Ca	K	Mg	Na	Si	Fl	Cl	NO_3	SO_4	Calculated Alkalinity
GL13-1	7/16/2013 8:10	8.59	9.74	1.84	150	63.11	23.24	6.36	38.12	38.67	0.70	18.24	0.85	19.67	141.17
GL13-2	7/16/2013 11:00	8.82	10.98	1.92	175	65.99	25.72	6.33	38.77	44.68	2.86	16.65	0.82	21.16	146.46
GL13-3	7/16/2013 14:00	8.70	11.54	NA	150	61.88	23.10	6.43	40.20	32.96	0.67	20.58	1.43	21.68	133.87
GL13-4	7/16/2013 17:00	8.70	9.44	NA	150	56.32	21.61	6.89	33.53	27.25	0.73	14.71	0.81	18.27	128.76
GL13-5	7/16/2013 20:00	8.65	10.04	3.28	150	50.31	15.65	4.87	28.65	27.84	0.64	7.53	0.45	15.63	114.79
GL13-6	7/16/2013 23:00	8.75	11.22	2.24	150	55.07	24.32	5.60	40.89	33.75	0.68	23.38	1.69	15.88	129.06
GL13-7	7/17/2013 2:00	8.73	8.82	2.80	150	55.96	18.77	5.52	29.67	32.96	0.58	11.53	<0.45	17.62	124.03
GL13-8	7/17/2013 5:00	8.84	10.32	1.60	175	59.65	27.05	5.94	38.90	34.34	<0.43	22.57	<0.45	19.35	135.86
GL13-9	7/17/2013 8:00	8.90	13	2.64	200	77.11	24.73	6.83	42.06	38.95	0.70	22.27	3.91	23.84	160.13
GL13-10	7/17/2013 11:00	8.51	12.66	2.40	150	61.76	22.14	6.46	33.64	34.54	0.74	15.23	1.16	23.85	127.40
GL13-11	7/17/2013 14:00	8.01	7.28	1.04	100	31.93	9.62	4.74	15.96	23.29	0.55	6.56	<0.45	15.56	60.69
GL13-13	7/17/2013 17:00	8.32	6.46	1.68	100	35.97	15.07	4.44	20.12	23.15	0.51	11.90	<0.45	14.14	75.32
GL13-14	7/17/2013 20:00	8.62	8.2	1.36	100	38.71	15.41	4.85	19.19	25.86	0.43	8.85	<0.45	14.99	82.45
GL13-15	7/17/2013 23:00	8.80	9.1	3.52	150	51.23	19.17	5.06	31.51	29.70	1.27	13.49	<0.45	9.54	129.42
GL13-16	7/18/2013 2:00	8.71	8.04	3.20	150	52.52	20.33	5.21	31.44	29.94	0.74	12.48	0.87	14.55	124.02
GL13-17	7/18/2013 5:00	8.53	10.66	2.88	150	58.17	21.66	6.06	32.69	33.77	0.87	14.59	0.76	17.66	131.26
GL13-18	7/18/2013 8:00	8.90	12.7	3.52	150	58.34	26.52	5.85	33.74	33.52	0.92	12.56	<0.45	21.50	132.18
GL13-19	7/18/2013 11:00	8.48	9.82	2.56	150	50.27	21.52	5.84	30.12	30.90	0.73	18.38	<0.45	19.98	104.80
GL13-20	7/18/2013 14:00	8.53	10.98	3.60	175	56.00	26.34	5.53	32.80	30.84	2.03	14.21	0.80	18.63	127.88
GL13-21	7/18/2013 17:00	8.66	9.42	3.60	150	48.92	22.88	4.68	30.15	28.08	0.61	13.82	0.66	16.16	112.80
GL13-22	7/18/2013 20:00	8.61	7.56	4.00	125	45.92	20.21	4.39	29.79	27.19	0.64	14.99	0.98	13.68	106.64
GL13-23	7/18/2013 23:00	8.60	7.06	3.20	100	44.93	19.53	4.35	33.33	26.04	0.50	34.89	0.60	12.51	90.43
GL13-24	7/19/2013 2:00	8.68	14.54	3.84	125	58.06	23.07	5.00	30.77	32.56	0.71	29.45	1.08	14.63	119.46
GL13-25	7/19/2013 5:00	8.27	9.42	2.56	150	50.26	23.64	4.83	28.40	30.22	<0.43	8.51	<0.45	14.96	123.76
GL13-26	7/19/2013 8:00	8.58	10.24	2.80	150	56.08	27.09	4.95	38.39	28.60	0.79	24.85	1.27	17.39	125.83
GL13-27	7/19/2013 11:00	8.70	10.5	2.64	150	59.22	28.32	5.32	35.07	30.39	0.80	18.63	2.05	20.54	129.90
GL13-28	7/19/2013 14:00	8.46	11.92	2.24	150	52.04	23.07	4.82	30.99	28.33	0.74	8.69	1.07	19.07	119.13
GL13-29	7/19/2013 17:00	8.35	11.66	3.44	125	51.33	25.01	4.73	30.98	26.10	0.69	16.41	1.50	16.31	116.88
GL13-30	7/19/2013 20:00	8.58	7.68	3.84	100	44.99	23.94	4.26	29.57	24.76	0.66	15.06	1.17	14.15	106.81
GL13-31	7/19/2013 23:00	8.58	7.42	2.96	100	42.73	24.46	4.05	29.26	23.92	0.64	14.57	0.77	13.32	104.67
GL13-32	7/20/2013 2:00	8.53	15.46	3.12	200	64.60	42.27	6.17	70.99	27.76	0.60	6.56	8.54	17.23	204.64
GL13-33	7/20/2013 5:00	8.03	8.62	3.68	150	55.74	24.52	4.85	30.50	26.84	0.75	10.08	1.78	16.88	129.83
GL13-34	7/20/2013 8:00	8.37	9.66	3.20	150	54.24	22.61	4.97	33.37	28.51	0.81	8.52	<0.45	20.50	124.06
GL13-35	7/20/2013 11:00	8.30	11.48	2.16	150	54.99	28.39	4.97	33.30	29.61	0.79	8.94	1.29	21.77	127.04
GL13-36	7/20/2013 14:00	8.39	9.94	2.88	150	51.93	24.12	4.84	32.49	28.51	0.79	8.71	1.28	20.74	117.89
GL13-37	7/20/2013 17:00	8.48	10.02	1.84	150	48.16	22.25	4.60	31.28	27.60	1.29	10.85	1.19	16.96	111.80
GL13-38	7/20/2013 20:00	8.69	9.06	2.00	125	42.10	18.12	4.06	29.09	24.59	0.66	7.35	<0.45	14.37	102.76
GL13-39	7/20/2013 23:00	8.12	6.62	1.44	100	42.13	12.60	5.49	22.80	29.38	<0.43	10.54	<0.45	19.25	81.60
GL13-40	7/21/2013 2:00	8.80	7.68	1.36	150	48.73	24.96	4.80	40.99	28.59	0.80	12.31	1.35	15.40	127.78
GL13-41	7/21/2013 5:00	8.20	7.22	3.68	150	45.80	21.11	4.45	34.07	25.88	0.74	12.08	1.20	15.56	110.55
GL13-42	7/21/2013 8:00	8.70	8.24	3.68	150	47.55	18.79	4.46	31.80	26.99	0.74	8.58	1.30	17.01	109.97
GL13-43	7/21/2013 11:00	8.42	8.76	2.72	150	46.89	20.93	4.51	33.33	26.81	0.76	8.28	0.72	17.63	112.03
GL13-44	7/21/2013 14:00	8.12	10.24	3.36	150	47.52	21.48	4.49	30.72	26.82	<0.43	9.04	<0.45	16.26	114.65
GL13-45	7/21/2013 17:00	8.32	8.08	2.64	150	44.42	17.05	4.03	29.55	24.22	1.01	10.22	1.36	14.10	102.73
GL13-46	7/21/2013 20:00	8.62	7.44	3.92	150	40.93	18.31	4.00	27.84	24.85	<0.43	7.66	<0.45	13.31	101.73

469